



Original Article

# High-Resolution Gene Expression Profiling Using RNA Sequencing in Patients With Inflammatory Bowel Disease and in Mouse Models of Colitis

Kristine Holgersen,<sup>a,d,e</sup> Burak Kutlu,<sup>b</sup> Brian Fox,<sup>b</sup> Kyle Serikawa,<sup>b</sup> James Lord,<sup>c</sup> Axel Kornerup Hansen,<sup>d</sup> Thomas Lindebo Holm<sup>e</sup>

<sup>a</sup>Novo Nordisk-LIFE *In Vivo* Pharmacology Centre, Frederiksberg, Denmark <sup>b</sup>NNRC-Molecular Immunology, Novo Nordisk Inc., Seattle, WA, USA <sup>c</sup>Benaroya Research Institute, Virginia Mason Medical Center, Seattle, WA, USA <sup>d</sup>Department of Veterinary Disease Biology, Faculty of Health and Medical Sciences, University of Copenhagen, Frederiksberg, Denmark <sup>e</sup>Department of Immunopharmacology, Novo Nordisk A/S, Maaloev, Denmark

Corresponding author: Kristine Holgersen, DVM, PhD, Department of Veterinary Disease Biology, University of Copenhagen, Thorvaldsensvej 57, stuen, E104, 1870 Frederiksberg, Denmark. Tel:+454-037-6347; Email: [krihol@sund.ku.dk](mailto:krihol@sund.ku.dk)

## Abstract

**Background and Aims:** Proper interpretation of data from preclinical animal studies requires thorough knowledge of the pathophysiology of both the human disease and animal models. In this study, the expression of inflammatory bowel disease [IBD]-associated genes was characterised in mouse models of colitis to examine the underlying molecular pathways and assess the similarity between the experimental models and human disease.

**Methods:** RNA sequencing was performed on colon biopsies from Crohn's disease [CD] patients, ulcerative colitis [UC] patients and non-IBD controls. Genes shown to be significantly dysregulated in human IBD were used to study gene expression in colons from a piroxicam-accelerated colitis interleukin-10 knockout [PAC IL-10 k.o.], an adoptive transfer [AdTr] and a dextran sulfate sodium [DSS] colitis mouse model.

**Results:** Of 115 literature-defined genes linked to IBD, 92 were significantly differentially expressed in inflamed mucosa of CD and/or UC patients compared with non-IBD controls. The most upregulated genes were shared by both diseases, including *REG1A*, *LCN2*, *NOS2*, *CXCL1-2*, and *S100A9*. Of those 92 IBD-associated genes, 71 [77%] were significantly dysregulated in PAC IL-10 k.o. mice, whereas 59 [64%] were significantly dysregulated in AdTr mice compared with wild-type controls. Some of the most upregulated genes, including *S100a8-9*, *Nos2*, and *Lcn2*, were shared by the colitis models and correlated with disease activity.

**Conclusions:** IBD and experimental murine colitis have a high degree of similarity in the colonic transcriptional profile, probably secondary to non-specific inflammatory processes. However, differences do exist between models, emphasising the need for careful selection and interpretation of qualified animal models in preclinical research.

**Keywords:** Experimental colitis; RNA sequencing; interleukin-10 knockout mouse

## 1. Introduction

Chronic immune-related disorders, like type 1 diabetes, multiple sclerosis, rheumatoid arthritis, psoriasis, and inflammatory bowel disease [IBD], are multifactorial, polygenic conditions and they have several risk loci shared among them.<sup>1</sup> IBD has one of the highest numbers of confirmed susceptibility loci, indicating a strong inherited component of the aetiology.<sup>2,3,4</sup> Recent genome-wide association studies [GWAS] have identified a total of 163 IBD susceptibility loci, which focus the attention on positional candidate genes involved in immunoregulation and microbial homeostasis.<sup>3,5</sup> The interplay between microbiota and genetics gives unique transcription profiles in the gut, and gene expression analyses provide insights into the transcriptional activity and functional molecular pathways underlying disease progression.<sup>6</sup> Therefore, deep sequencing analysis of the colon suggests hypotheses about the pathophysiological processes in IBD patients. GWAS emphasise a substantial overlap in the genetic risk loci between ulcerative colitis [UC] and Crohn's disease [CD],<sup>3</sup> and Granlund *et al.*<sup>7</sup> demonstrated a remarkable similarity in the mucosal gene expression pattern related to antimicrobial peptides and T helper [Th] cell activation. However, fundamental differences in the pathology of CD and UC exist. Whereas UC is characterised by diffuse inflammation confined to the mucosa of colon and rectum, the inflammation of CD is discontinuous, transmural and can affect the entire gastrointestinal tract. Also, CD patients often present complications like intestinal strictures, fistulas, and abscesses.<sup>8,9,10</sup> Based on the mucosal expression of transcription factors and cytokines, CD has been associated with a dysregulated Th1/Th17 response,<sup>9</sup> whereas UC has been associated with a Th2/natural killer T cell response.<sup>8</sup>

Murine models are extensively used in the preclinical research of IBD. Two commonly used experimental models are the dextran sulfate sodium [DSS]-induced colitis mouse and the adoptive T cell [CD4<sup>+</sup>CD45RB<sup>high</sup> or CD4<sup>+</sup>CD25<sup>+</sup>] transfer [AdTr] mouse. DSS treatment causes non-specific injury to the colonic epithelium, leading to acute inflammation and an erosive histological phenotype, which resembles UC.<sup>11,12,13</sup> In the AdTr model, chronic colitis develops due to an expansion of transferred naïve CD4<sup>+</sup> T cells from wild-type [WT] mice to immunodeficient recipients. In the absence of regulatory T cells, the naïve T cells convert into pathogenic Th1/Th17 effector cells and CD-like histopathological lesions develop, including epithelial hyperplasia and focal transmural inflammation.<sup>14,15,16</sup> We have previously demonstrated how piroxicam-accelerated colitis in interleukin-10 knockout [PAC IL-10 k.o.] mice mimics the pathological features of IBD, particularly CD, and shows responsiveness to known IBD therapeutics.<sup>17,18</sup> The pathogenesis of the PAC IL-10 k.o. model is heterogeneous, and the innate immune response and commensal microflora seem to play a major role.<sup>17,18</sup> However, the underlying molecular pathways have not been thoroughly investigated.

To qualify various suggested IBD biomarkers, we reviewed the literature and found 115 genes linked to the disease. In this study, we quantified the expression of those selected genes in UC and CD patients. With a general focus on the PAC IL-10 k.o. model, genes that were shown to be significantly differentially expressed in IBD patients were used to describe the transcriptional profiles in the colon of three experimental colitis models. The present data allowed us to further characterise the molecular pathways underlying disease development, and by comparison assess the similarity between the animal models and human disease.

## 2. Materials and Methods

### 2.1. Human material

All human samples and clinical data were obtained from a biorepository at the Benaroya Research Institute, Seattle, WA. This biorepository contains de-identified specimens, and abstracted demographic and clinical information from consenting donors who received their medical care at the Virginia Mason Medical Center [VMMC]. It has been generated and maintained in compliance with a protocol approved by the Institutional Review Board [IRB] at VMMC, in accordance with the Declaration of Helsinki. Patients previously diagnosed with UC or CD, undergoing colonoscopy as part of their routine medical care, as well as non-IBD controls undergoing routine screening colonoscopy, were included in the study. Colon tissue was assessed as inflamed or non-inflamed by the performing endoscopist based on endoscopic findings at the time of collection. Jumbo forceps colon biopsies for RNA extraction were snap-frozen on dry ice at the bedside immediately *ex vivo*. A second biopsy, from a site immediately adjacent to the first, was then frozen at the bedside in Optimal Cutting Temperature (OCT) compound for histology. Sections of the latter were stained with haematoxylin and eosin [H&E] and evaluated by an independent pathologist to confirm the presence or absence of inflammation in the samples. Only inflamed tissue from UC and CD patients was used for gene expression analyses. The sample collection consisted of 9 CD, 10 UC [7 from colon, 3 from rectum], and 15 non-IBD control colon biopsies. Demographic and clinical details of the patients and controls are provided in [Supplementary Table 1](#), available as Supplementary data at *ECCOJC* online. None of the patients on prednisone was taking > 10 mg a day at the time of sampling.

### 2.2. Mice

All mouse experiments were carried out in accordance with the European Communities Council Directive 2010/63/EU for the protection of animals used for experimental purposes and were approved by the Danish Animal Experiments Inspectorate, Ministry of Food, Agriculture and Fisheries, Denmark, as well as by the internal Ethical Review Committee at Novo Nordisk A/S. B6.129P2-*Il10<sup>tm1Cgn</sup>/J* [IL-10 k.o.] mice and C57BL/6J wild-type [WT] mice were obtained from Charles River Laboratories [Sulzfeld, Germany] in accordance with a licence agreement with MCG [Munich, Germany]. C.B-17 severe combined immunodeficiency [SCID] mice and BALB/c WT mice were purchased from Taconic M&B [Ry, Denmark]. Female mice, 8–12 weeks old, were used in all the studies. The mice were housed at Novo Nordisk A/S, Maaloev, Denmark, and kept under barrier-protected conditions free of agents listed in FELASA guidelines.<sup>19</sup> They were housed with 10 mice per cage and a 12-h light/dark cycle. The bedding was changed weekly, and in order to ensure a homogeneous microbial environment, dirty cage bedding was transferred between cages. The clinical status of the mice was evaluated three times weekly by percentage weight change and faecal consistency. Faecal consistency was assessed on a scale of 0–4, with 0 representing a hard, firm stool and 4 representing a liquid stool with no firm consistency. Mice were sacrificed by cervical dislocation if their weight loss exceeded 20% of the initial weight or if they had a morbid appearance.

### 2.3. Induction of colitis in animal models

For induction of the PAC IL-10 k.o. model, IL-10 k.o. mice [*n* = 12] had unrestricted access to piroxicam [Sigma Aldrich, Broendby, Denmark] 200 ppm homogenized in 1324 Altromin diet [Altromin, Lage, Germany] from Day 0 until termination, at Day 10 of the

experiment. Both healthy IL-10 k.o. mice [ $n = 3$ ] and C57BL/6J mice [ $n = 3$ ] were used to establish a control baseline gene expression level for the PAC IL-10 k.o. mouse model. The AdTr model was conducted as previously described.<sup>14</sup> In brief, a CD4<sup>+</sup>CD25<sup>-</sup> cell subset was prepared from BALB/c splenocytes by positive selection of CD4<sup>+</sup> T cells using Dynabeads and DETACHaBEAD [Dynal, Oslo, Norway] followed by a negative selection of CD4<sup>+</sup>CD25<sup>+</sup> cells using the CD25 MicroBead kit [Miltenyi Biotech, Bergisch Gladbach, Germany]. The purity of the cells was evaluated by flow cytometric analysis [FACS] before reconstitution. Immunodeficient SCID recipient mice [ $n = 9$ ] were reconstituted by injection of 300 000 CD4<sup>+</sup>CD25<sup>-</sup> T cells intraperitoneally. Peripheral blood from the mice was analysed by FACS 4 weeks after transfer, and only mice with CD4<sup>+</sup> T cells were included. The AdTr mice were sacrificed between Days 28–37 of the experiment, when colitis is known to be established.<sup>14</sup> Both healthy BALB/c [ $n = 5$ ] and SCID [ $n = 4$ ] were used as controls for the AdTr mouse model. DSS colitis was induced in BALB/c mice [ $n = 6$ ] by 4% DSS [ICN Biomedicals, OH] dissolved in de-ionised water, administered to the mice *ad libitum* in water bottles, from Day 0 until Day 5 of the experiment. From Day 5, the mice received de-ionised water without DSS. The DSS-induced colitis mice were sacrificed at Day 8 of the experiment. Healthy BALB/c mice [ $n = 7$ ] were used as controls for the DSS mouse model.

## 2.4. Post-mortem analyses

Mice were sacrificed by cervical dislocation, and caecum, colon, and rectum were excised. The length of the colon was measured from the caeco-colonic junction to the anus. The colon was rinsed with phosphate-buffered saline and weighed. The colonic weight:length [W:L] ratio [mg/cm] was used as a macroscopic, objective parameter to verify the presence of established colitis, since it is known to correlate with the histology score, especially in the AdTr model.<sup>14,17</sup> The proximal one-third of the colon was removed and the remaining two-thirds of colon bisected longitudinally. One-half of the colon was processed for histological analysis and the other half of the colon was collected for RNA isolation. The colon segment selected for mRNA sequencing [RNAseq] depended on the predominant disease location in the particular model. All samples were collected in areas previously identified as representing continuous high-grade inflammation. Thus, a whole colon segment was used for RNAseq analysis in the PAC IL-10 k.o. model, whereas a transverse colon segment was used in the AdTr model, and a distal colon segment in the DSS model.

## 2.5. Histological examination

Histological analysis was performed on colon tissue from PAC IL-10 k.o. mice and DSS mice in order to verify the presence of colitis. Colon tissue was fixed in 4% paraformaldehyde [VWR-Bie & Berntsen, Herlev, Denmark] for approximately 24 h and then transferred to 70% ethanol and stored at 4°C until processed. The samples were processed in a Leica Asp300S histoprocessor [Leica Microsystems, Ballerup, Denmark] overnight, embedded in paraffin blocks using a Shandon Histocentre 3 [Thermo Electron Corporation, Marietta, Ohio] and sectioned in a Leica Microtome RM 2165 [Leica Microsystems, Ballerup, Denmark]. Subsequently, the slides were H&E-stained for light-microscopic examination. A proximal [~2 cm] and distal [~3 cm] colon segment were evaluated in a blinded fashion by two persons. In the DSS model, the four histological features were assessed—ulceration, crypt distortion, loss of mucin, and cell infiltration—and given a score between 0 and 3 [normal = 0; mild = 1; moderate = 2, severe = 3]. The PAC IL-10

k.o. model was histologically evaluated by the four features—cell infiltration, hyperplasia, ulceration, and area involved, as previously described.<sup>17</sup> The total colonic histology score was the sum of all scores including both the proximal and distal segment; i.e. total score ranging from 0 to 24.

## 2.6. RNA extraction

Colon tissue for RNAseq analysis was transferred to individual tubes containing RNeasy lysis buffer [Ambion, Austin, TX], snap-frozen and stored at -80°C until processed. The samples were added to QIAzol [Qiagen, Valencia, CA] or RLT plus  $\beta$ -mercaptoethanol [BME] buffer [Qiagen, Valencia, CA] for lysis of the tissue. The samples were homogenized and chloroform or acid phenol:chloroform was added to the samples containing QIAzol or RLT plus BME, respectively. The samples were shaken and centrifuged and 70% ethanol was added to the supernatant. The total mRNA was isolated from the tissue extract using a Qiagen RNeasy Mini kit protocol [Qiagen, Valencia, CA] with RNase-free DNase treatment [Ambion, Austin, TX]. The total RNA was re-suspended in 250  $\mu$ l of RNase/DNase-free water. RNA quantitation was performed using a NanoDrop spectrometer [Thermo Fisher Scientific, Wilmington, DE] for protein concentration > 10 ng/ml or via Ribogreen RNA assay Kit [Life Technologies, Carlsbad, CA] for lower concentrations. RNA quality was analysed by a Bioanalyzer [Agilent Technologies, Santa Clara, CA] which assessed the 28S/18S ratio of the ribosomal RNA bands. Samples were only used in subsequent analyses if the RNA Integrity Number [RIN] was greater than 6.

## 2.7. RNA sequencing analysis

For preparation of the RNA sequence libraries, 100 ng of total RNA was sequenced per sample using the Illumina TruSeq Sample Prep Kit and HiSeq 2000 system [Illumina, San Diego, CA] according to the manufacturer's instructions. The analysis was run at a multiplexing level sufficient to generate 10–25 million reads per sample. The reads were aligned to the appropriate genome using the Tuxedo suite [Bowtie/TopHat/Cufflinks suite]. Quality control of the sequencing data was accomplished using the ShortRead package in the R/Fastx toolkit. Aligned reads were converted to Reads per Kilobase per Million [RPKM] values, calculated by the Ensemble transcript models. After applying the RNAseq methods, 115 genes suggested to be involved in gut homeostasis and inflammation were chosen for further study. The colonic gene expression of CD and UC patients was compared with non-IBD controls and presented in a table showing the  $\log_2$ -transformed fold change [FC] and adjusted [Adj]  $p$ -value. Significantly differentially expressed genes are presented in Table 1 and non-differentially expressed genes are presented in Supplementary Table 2, available as Supplementary data at ECCOJC online. Genes shown to be significantly up- or down-regulated in IBD patients were used to assess the transcriptional profiles of the PAC IL-10 k.o., AdTr, and DSS colitis models. The gene expression pattern of the experimental colitis models was compared with their respective WT controls and are presented in a table showing FC and Adj  $p$ -value [Table 2]. Moreover, the transcriptional profiles of the experimental colitis models were presented in heat maps, in which each gene expression [row] was standardised [row mean subtracted for each row and divided by standard deviation] across all mice [Figures 4–6]. This allowed us to compare the gene expression profiles between all the different genetic strains. Within the PAC IL-10 k.o. cohort and the AdTr cohort, mice were organised according to degree of colitis, i.e. W:L ratio. The mouse with the highest W:L ratio was located to the left, and the mouse with the lowest W:L ratio was located to the right of the heat maps.

**Table 1.** Significantly differentially expressed genes in IBD patients.

Gene symbol	Ensembl gene id	CD [FC]	Adj <i>p</i> -value	UC [FC]	Adj <i>p</i> -value	Function	References
TNF	ENSG00000232810	0.76	0.02	1.39	<0.01	Cytokines and receptors	7,20
IFNG	ENSG00000111537	0.49	0.02	0.6	0.01	Cytokines and receptors	7,21,22
IL1B	ENSG00000125538	2.52	0.01	2.79	<0.01	Cytokines and receptors	7,23,24,25
IL2RA	ENSG00000134460	0.62	0.02	1.5	0.01	Cytokines and receptors	7,26
IL6	ENSG00000136244	0.81	ns	1.23	0.01	Cytokines and receptors	7,20,23,25
IL12B	ENSG00000113302	0.11	ns	0.1	0.01	Cytokines and receptors	27,28
IL16	ENSG00000172349	0.6	ns	1.39	0.01	Cytokines and receptors	29
IL17A	ENSG00000112115	0.45	ns	0.61	0.02	Cytokines and receptors	7,28
IL17F	ENSG00000112116	0.35	ns	0.17	0.01	Cytokines and receptors	7
IL18R1	ENSG00000115604	0.5	0.02	0.8	0.01	Cytokines and receptors	30
IL21	ENSG00000138684	0.12	ns	0.52	0.02	Cytokines and receptors	7,31
IL21R	ENSG00000103522	0.8	0.03	1.68	0.01	Cytokines and receptors	31
IL22	ENSG00000127318	0.32	0.03	0.43	0.02	Cytokines and receptors	7,32
IL23A	ENSG00000110944	0.7	0.02	1.25	0.01	Cytokines and receptors	7,27
IL23R	ENSG00000162594	-0.43	0.05	-0.63	0.01	Cytokines and receptors	33
IL33	ENSG00000137033	1.12	0.01	1.97	<0.01	Cytokines and receptors	28,34
LTB	ENSG00000227507	1.38	0.02	2.39	<0.01	Cytokines and receptors	6,26
STAT1	ENSG00000115415	1.26	0.01	1.46	<0.01	Intracellular signaling/ cell surface markers	7
STAT3	ENSG00000168610	0.66	0.02	0.78	<0.01	Intracellular signaling/ cell surface markers	7,27
STAT5A	ENSG00000126561	0.51	0.02	0.82	0.01	Intracellular signaling/ cell surface markers	7
TYK2	ENSG00000105397	0.22	ns	0.27	0.03	Intracellular signaling/ cell surface markers	6
JAK2	ENSG00000096968	0.59	0.03	0.94	<0.01	Intracellular signaling/ cell surface markers	27,33
PTPN22	ENSG00000134242	0.22	ns	0.59	0.02	Intracellular signaling/ cell surface markers	35
CD4	ENSG00000010610	0.63	ns	1.51	<0.01	Intracellular signaling/ cell surface markers	36,37
CTLA4	ENSG00000163599	1.23	0.02	2.06	<0.01	Intracellular signaling/ cell surface markers	38,39
CD80	ENSG00000121594	0.28	ns	0.79	0.01	Intracellular signaling/ cell surface markers	40
CD86	ENSG00000114013	0.66	0.03	1.47	<0.01	Intracellular signaling/ cell surface markers	22,40
TBX21	ENSG00000073861	0.42	0.02	0.72	0.01	Intracellular signaling/ cell surface markers	7,28
GATA3	ENSG00000107485	0.25	ns	0.42	0.01	Intracellular signaling/ cell surface markers	7,28,34
KLRK1	ENSG00000213809	0.25	ns	0.51	0.01	Intracellular signaling/ cell surface markers	41
CCR2	ENSG00000121807	0.28	ns	0.76	0.01	Chemokines and receptors	28,42
CCR7	ENSG00000126353	1.21	0.03	2.11	<0.01	Chemokines and receptors	7,30,43
CCR6	ENSG00000112486	0.66	0.05	1.59	<0.01	Chemokines and receptors	7,28
CCL2	ENSG00000108691	1.13	0.02	1.94	<0.01	Chemokines and receptors	27,43,44,45
CCL3	ENSG00000006075	0.82	ns	0.87	0.01	Chemokines and receptors	43,45
CCL4	ENSG00000129277	0.48	0.02	1.18	<0.01	Chemokines and receptors	43,45
CCL11	ENSG00000172156	0.79	ns	1.37	<0.01	Chemokines and receptors	28,43
CCL17	ENSG00000102970	0.53	0.03	1.18	0.01	Chemokines and receptors	28
CCL20	ENSG00000115009	2.24	0,01	2.59	<0.01	Chemokines and receptors	26,27,43
CXCR1	ENSG00000163464	0.25	ns	0.51	0.02	Chemokines and receptors	30,46
CXCR3	ENSG00000186810	0.32	ns	0.67	0.01	Chemokines and receptors	7,30
CXCL1	ENSG00000163739	3.55	0.01	4.41	<0.01	Chemokines and receptors	23,27,43,46
CXCL2	ENSG00000081041	2.43	0.01	2.41	<0.01	Chemokines and receptors	23,27,43,46
CXCL5	ENSG00000163735	1.72	0.02	1.32	<0.01	Chemokines and receptors	24,43
CXCL10	ENSG00000169245	1.73	0.02	2.55	<0.01	Chemokines and receptors	27,43,44
CXCL9	ENSG00000138755	1.81	0.02	2.49	<0.01	Chemokines and receptors	27,43
CXCL12	ENSG00000107562	0.21	ns	0.82	<0.01	Chemokines and receptors	24
CXCL13	ENSG00000156234	1.33	ns	3.35	<0.01	Chemokines and receptors	27,43,46
CX3CL1	ENSG00000006210	0.71	0.01	0.78	0.01	Chemokines and receptors	43
SELE	ENSG00000007908	0.7	0.03	1.15	0.01	Adhesion	24,43
ICAM1	ENSG00000090339	1.32	0.01	1.94	<0.01	Adhesion	28,43



Table 1. Continued

Gene symbol	Ensembl gene id	CD [FC]	Adj <i>p</i> -value	UC [FC]	Adj <i>p</i> -value	Function	References
VCAM1	ENSG00000162692	1.04	0.05	2.44	<0.01	Adhesion	28,43
MADCAM1	ENSG00000099866	0.81	0.02	1.59	0.01	Adhesion	43
CD44	ENSG00000026508	0.88	0.01	1.31	<0.01	Adhesion	24,47
DEFB1	ENSG00000164825	-1.67	<0.01	-2.42	<0.01	Mucosal barrier	7,24,48
DEFB4A	ENSG00000171711	1	ns	2.18	<0.01	Mucosal barrier	7,48
MUC1	ENSG00000185499	1.93	<0.01	1.16	0.03	Mucosal barrier	28
TFF1	ENSG00000160182	1.9	<0.01	2.76	<0.01	Mucosal barrier	23,24
VIM	ENSG00000026025	0.56	ns	1.25	<0.01	Mucosal Barrier	24
CLDN1	ENSG00000163347	0.96	0.02	1.29	<0.01	Mucosal barrier	24,49
OCLN	ENSG00000197822	-0.3	ns	-0.5	0.04	Mucosal barrier	50
PTGS2	ENSG00000073756	0.65	ns	1.27	0.02	Mucosal barrier	24,28
PPARG	ENSG00000132170	-0.92	0.01	-1.62	<0.01	Mucosal barrier	7,24
CDX2	ENSG00000165556	-0.63	ns	-1.65	<0.01	Mucosal barrier	51
MMP3	ENSG00000149968	2.29	0.03	3.74	<0.01	Tissue remodelling	23,26,52,53
MMP7	ENSG00000137673	1.69	0.02	2.9	<0.01	Tissue remodelling	26,52,54
MMP9	ENSG00000100985	1.73	0.01	2.81	<0.01	Tissue remodelling	23,52,54
MMP14	ENSG00000157227	0.79	<0.01	0.91	<0.01	Tissue remodelling	53
MMP10	ENSG00000166670	1.08	ns	1.83	<0.01	Tissue remodelling	24,52
TIMP1	ENSG00000102265	1.94	<0.01	2.8	<0.01	Tissue remodelling	23,24,52,54
COL1A2	ENSG00000164692	0.97	0.03	1.72	<0.01	Tissue remodelling	23,24
COL6A3	ENSG00000163359	1.05	0.01	1.82	<0.01	Tissue remodelling	23
EGR3	ENSG00000179388	0.65	ns	1.36	<0.01	Tissue remodelling	24
VEGFC	ENSG00000150630	0.47	0.01	0.82	<0.01	Tissue remodelling	24,55
TLR2	ENSG00000137462	0.4	0.02	0.85	<0.01	Bacterial sensing	56,57
TLR4	ENSG00000136869	0.35	ns	0.93	<0.01	Bacterial sensing	26,57
NOD2	ENSG00000167207	0.45	0.01	0.68	<0.01	Bacterial sensing	27
LTF	ENSG000000012223	1.06	ns	2.75	<0.01	Bacterial sensing	26,48
LYZ	ENSG00000090382	1.64	<0.01	2.47	<0.01	Bacterial sensing	7,23,48
LCN2	ENSG00000148346	4.12	<0.01	4.66	<0.01	Bacterial sensing	23,26,48
REG1A	ENSG00000115386	4.54	0.01	4.66	<0.01	Bacterial sensing	23,24
CD55	ENSG00000196352	2.03	<0.01	2.59	<0.01	Complement system	58
C3	ENSG00000125730	1.34	0.04	2.8	<0.01	Complement system	59
C5	ENSG00000106804	0.15	ns	0.18	0.02	Complement system	48
CR2	ENSG00000117322	1.31	ns	2.96	<0.01	Complement system	6
S100A8	ENSG00000143546	1.39	0.03	2.29	<0.01	S100 family	26,48
S100A9	ENSG00000163220	2.25	0.01	3.47	<0.01	S100 family	26,48
ABCB1	ENSG00000085563	-1.44	0.01	-1.71	<0.01	Multidrug resistance	23,26
CASP1	ENSG00000137752	1.59	<0.01	1.46	<0.01	Apoptosis	24,28
ISG15	ENSG00000187608	1.17	<0.01	1.23	<0.01	Ubiquitin-like protein	47
NOS2	ENSG000000007171	3.02	0.01	3.8	<0.01	Nitric oxide synthase	23,48
VWF	ENSG00000110799	1.14	0.01	1.33	<0.01	Haemostasis	23,24

Expression profile of the 92 genes, shown to be significantly up- or downregulated in inflamed colonic mucosa of CD or UC patients. Data represent gene expression in CD [*n* = 9] or UC [*n* = 10] patients compared with non-IBD controls [*n* = 15]. RNAseq was performed on colon samples and the *p*-value was adjusted for multiple testing. Fold change values have been transformed to log<sub>2</sub>-scale [FC], thus positive FC values indicate an upregulation, whereas negative FC values indicate a downregulation in gene expression. An adjusted [Adj] *p*-value ≤ 0.05 was considered significant. CD, Crohn's disease; UC, ulcerative colitis; FC, fold change; ns, non-significant.

2.8. Statistical analysis

In the mouse studies, GraphPad Prism version 6.04 was used for all statistical analyses. Statistical significance of differences between normally distributed, parametric data from two groups was evaluated using an unpaired Student's *t* test. The comparison of not normally distributed data from two groups was performed using a non-parametric Mann-Whitney *U* test. Statistical significance between more than two groups was evaluated by a one-way ANOVA [parametric] or Kruskal-Wallis test [non-parametric] with Holm-Sidak's or Dunn's multiple comparison test, respectively. A Spearman's correlation coefficient was calculated for analysis of correlation between colonic W:L ratio and gene expression level in the PAC IL-10 k.o. and AdTr models. Differences were considered

statistically significant when *p*-value < 0.05 and significance levels were assigned \* for *p* < 0.05, \*\* for *p* < 0.01, and \*\*\* for *p* < 0.001. Statistical significance of the RNAseq data was analysed using Student's *t* test and *p*-values were adjusted for multiple testing by Benjamini-Hochberg method. An Adj *p*-value ≤ 0.05 was considered statistically significant.

3. Results

3.1. Transcriptional profiles in the colon of IBD patients.

By RNAseq analysis the expression of 115 genes, suggested to be relevant in IBD pathogenesis, was quantified in colon biopsies

**Table 2.** Expression profile of IBD-associated genes in experimental colitis models

Gene symbol	Ensembl gene id	PAC IL-10 k.o. model, [FC]	Adj <i>p</i> -value	AdTr model, [FC]	Adj <i>p</i> -value	DSS model, [FC]	Function
Tnf	ENSMUSG00000024401	2.85	<0.01	3.21	<0.01	2.68	Cytokines and receptors
Ifng	ENSMUSG00000055170	2.2	<0.01	1.3	<0.01	0.9	Cytokines and receptors
Il1b	ENSMUSG00000027398	3.46	<0.01	2.21	<0.01	3.36	Cytokines and receptors
Il2ra	ENSMUSG00000026770	0.73	<0.01	0.24	ns	0.99	Cytokines and receptors
Il6	ENSMUSG00000025746	0.84	<0.01	0.1	0.03	0.75	Cytokines and receptors
Il12b	ENSMUSG00000004296	0.81	<0.01	0.35	0.03	0.23	Cytokines and receptors
Il16	ENSMUSG00000001741	0.45	<0.01	-0.16	ns	0.94	Cytokines and receptors
Il17a	ENSMUSG00000025929	1.05	<0.01	0.29	0.02	0.09	Cytokines and receptors
Il17f	ENSMUSG000000041872	0.63	<0.01	0.24	0.04	0.34	Cytokines and receptors
Il18r1	ENSMUSG00000026070	0.95	<0.01	1.14	<0.01	-0.65	Cytokines and receptors
Il21	ENSMUSG000000027718	0.19	<0.01	0.05	ns	0	Cytokines and receptors
Il21r	ENSMUSG00000030745	1.31	<0.01	-0.07	ns	2.12	Cytokines and receptors
Il22	ENSMUSG00000074695	1.08	0.01	0.34	0.03	0	Cytokines and receptors
Il23a	ENSMUSG00000025383	-0.02	ns	0.04	ns	0.05	Cytokines and receptors
Il23r	ENSMUSG00000049093	0.17	<0.01	-0.02	ns	0.33	Cytokines and receptors
Il33	ENSMUSG00000024810	0.97	0.01	-0.47	ns	1.21	Cytokines and receptors
Ltb	ENSMUSG00000024399	0.89	0.01	0.13	ns	1.17	Cytokines and receptors
Stat1	ENSMUSG000000026104	2.57	<0.01	2.36	<0.01	2.49	Intracellular signaling/ cell surface markers
Stat3	ENSMUSG000000004040	0.57	<0.01	0.32	0.03	0.76	Intracellular signaling/ cell surface markers
Stat5a	ENSMUSG000000004043	0.15	ns	-0.04	ns	0.38	Intracellular signaling/ cell surface markers
Tyk2	ENSMUSG000000032175	-0.02	ns	-0.01	ns	-0.14	Intracellular signaling/ cell surface markers
Jak2	ENSMUSG00000024789	0.45	<0.01	0.37	ns	0.14	Intracellular signaling/ cell surface markers
Ptpn22	ENSMUSG000000027843	1.09	<0.01	0.75	0.03	1.2	Intracellular signaling/ cell surface markers
Cd4	ENSMUSG000000023274	0.79	<0.01	1	0.02	1.5	Intracellular signaling/ cell surface markers
Ctla4	ENSMUSG00000026011	1.76	<0.01	0.51	0.02	1	Intracellular signaling/ cell surface markers
Cd80	ENSMUSG000000075122	0.59	<0.01	0.42	0.02	0.47	Intracellular signaling/ cell surface markers
Cd86	ENSMUSG000000022901	1.09	<0.01	0.39	ns	0.22	Intracellular signaling/ cell surface markers
Tbx21	ENSMUSG00000001444	0.64	<0.01	0.69	0.01	1.45	Intracellular signaling/ cell surface markers
Gata3	ENSMUSG000000015619	0.67	<0.01	0.5	0.02	1.27	Intracellular signaling/ cell surface markers
Klrl1	ENSMUSG000000030149	1.09	<0.01	0.71	<0.01	1.04	Intracellular signaling/ cell surface markers
Ccr2	ENSMUSG000000049103	2.22	<0.01	1.22	<0.01	1.39	Chemokines and receptors
Ccr7	ENSMUSG000000037944	0.68	0.04	-0.3	ns	1.53	Chemokines and receptors
Ccr6	ENSMUSG000000040899	0.07	ns	-0.59	0.02	2.52	Chemokines and receptors
Ccl2	ENSMUSG000000035385	2.48	<0.01	2.43	<0.01	2.46	Chemokines and receptors
Ccl3	ENSMUSG000000000982	1.41	<0.01	0.76	0.02	-1.66	Chemokines and receptors
Ccl4	ENSMUSG000000018930	1.86	<0.01	1.39	<0.01	2.08	Chemokines and receptors
Ccl11	ENSMUSG000000020676	0.83	0.01	1	0.01	0.97	Chemokines and receptors
Ccl17	ENSMUSG000000031780	0.13	ns	1.21	<0.01	-0.81	Chemokines and receptors
Ccl20	ENSMUSG000000026166	0.28	ns	1.17	<0.01	-0.81	Chemokines and receptors
Cxcr1	ENSMUSG000000048480	0.09	0.01	0.07	ns	0.29	Chemokines and receptors
Cxcr3	ENSMUSG000000050232	0.84	<0.01	1	<0.01	1.08	Chemokines and receptors
Cxcl1	ENSMUSG000000029380	2.89	<0.01	2.37	<0.01	3.53	Chemokines and receptors
Cxcl2	ENSMUSG000000058427	2.57	<0.01	1.78	<0.01	1.69	Chemokines and receptors
Cxcl5	ENSMUSG000000029371	5.2	<0.01	3.77	<0.01	3.7	Chemokines and receptors
Cxcl10	ENSMUSG000000034855	4.22	<0.01	3.86	<0.01	3.11	Chemokines and receptors
Cxcl9	ENSMUSG000000029417	4.5	<0.01	4.59	<0.01	3.83	Chemokines and receptors
Cxcl12	ENSMUSG000000061353	-0.17	0.03	-0.45	ns	0.73	Chemokines and receptors
Cxcl13	ENSMUSG000000023078	1.2	0.01	1.11	0.03	3.74	Chemokines and receptors
Cx3cl1	ENSMUSG000000031778	-0.6	<0.01	-0.4	ns	-1.25	Chemokines and receptors

Table 2. Continued

Gene symbol	Ensembl gene id	PAC IL-10 k.o. model, [FC]	Adj <i>p</i> -value	AdTr model, [FC]	Adj <i>p</i> -value	DSS model, [FC]	Function
Sele	ENSMUSG00000026582	0.17	0.03	0.02	ns	0.31	Adhesion
Icam1	ENSMUSG00000037405	2.22	<0.01	1.58	<0.01	2.53	Adhesion
Vcam1	ENSMUSG00000027962	1.27	<0.01	1.17	<0.01	1.02	Adhesion
Madcam1	ENSMUSG00000020310	0.74	<0.01	-0.34	ns	0.14	Adhesion
Cd44	ENSMUSG00000005087	0.25	ns	0.6	<0.01	0.63	Adhesion
Defb1	ENSMUSG00000044748	-0.1	ns	-0.29	ns	-0.2	Mucosal barrier
Defb4	ENSMUSG00000059230	-0.12	ns	0	ns	1.14	Mucosal barrier
Muc1	ENSMUSG00000042784	1.63	<0.01	1.43	<0.01	-0.54	Mucosal barrier
Tff1	ENSMUSG00000024032	nd	ns	nd	0.04	nd	Mucosal barrier
Vim	ENSMUSG00000026728	-0.15	ns	-0.53	0.04	0.21	Mucosal barrier
Cldn1	ENSMUSG00000022512	-0.43	<0.01	-0.43	<0.01	1.2	Mucosal barrier
Ocln	ENSMUSG00000021638	-0.71	<0.01	-1.03	ns	-0.15	Mucosal barrier
Ptgs2	ENSMUSG00000032487	0.96	<0.01	0.14	ns	0.28	Mucosal barrier
Pparg	ENSMUSG00000000440	0.71	ns	0.32	ns	0.49	Mucosal barrier
Cdx2	ENSMUSG00000029646	0.15		-0.51		-0.94	Mucosal barrier
Mmp3	ENSMUSG00000043613	3.13	<0.01	2.34	<0.01	3.11	Tissue remodelling
Mmp7	ENSMUSG00000018623	3.74	<0.01	3.49	<0.01	0.74	Tissue remodelling
Mmp9	ENSMUSG00000017737	2.14	<0.01	0.98	<0.01	1.83	Tissue remodelling
Mmp14	ENSMUSG00000000957	0.41	<0.01	0.16	ns	0.27	Tissue remodelling
Mmp10	ENSMUSG00000047562	3.48	<0.01	1.46	0.01	2.87	Tissue remodelling
Timp1	ENSMUSG00000001131	2.16	<0.01	1.06	<0.01	2.6	Tissue remodelling
Col1a2	ENSMUSG00000029661	-0.13	ns	-0.74	<0.01	-0.13	Tissue remodelling
Col6a3	ENSMUSG00000048126	-0.96	<0.01	-0.77	<0.01	-0.38	Tissue remodelling
Egr3	ENSMUSG00000033730	0.32	ns	-0.15	ns	2.12	Tissue remodelling
Vegfc	ENSMUSG00000031520	-0.24	0.05	0.17	ns	-0.41	Tissue remodelling
Tlr2	ENSMUSG00000027995	1	<0.01	1.37	<0.01	1.23	Bacterial sensing
Tlr4	ENSMUSG00000039005	0.64	<0.01	0.32	ns	0.61	Bacterial sensing
Nod2	ENSMUSG00000055994	0.84	<0.01	1.22	<0.01	1.94	Bacterial sensing
Ltf	ENSMUSG00000032496	1.75	ns	4.31	<0.01	1.84	Bacterial sensing
Lyz1	ENSMUSG00000006915	0.17	ns	0.77	ns	-0.72	Bacterial sensing
Lcn2	ENSMUSG00000026822	3.79	<0.01	4.82	<0.01	2.63	Bacterial sensing
Reg1	ENSMUSG00000059654	1.81	ns	-3.21	ns	0	Bacterial sensing
Cd55	ENSMUSG00000026399	0.01	ns	-0.28	ns	0.21	Complement system
C3	ENSMUSG00000024164	1.93	<0.01	2.33	<0.01	1.51	Complement system
C5	ENSMUSG00000026874	-0.25	0.05	-0.02	ns	0.09	Complement system
Cr2	ENSMUSG00000026616	-0.14	ns	-1.4	<0.01	1.44	Complement system
S100a8	ENSMUSG00000056054	6.29	<0.01	7.54	<0.01	6.11	S100 family
S100a9	ENSMUSG00000056071	5.92	<0.01	6.92	<0.01	5.46	S100 family
Abcb1a	ENSMUSG00000040584	-2.19	<0.01	-2.41	<0.01	-2.65	Multidrug resistance
Casp1	ENSMUSG00000025888	0.41	ns	0.67	<0.01	0.94	Apoptosis
Isg15	ENSMUSG00000035692	1.97	0.02	1.67	<0.01	2.42	Ubiquitin-like protein
Nos2	ENSMUSG00000020826	5.24	<0.01	6.28	<0.01	5.29	Nitric oxide synthase
Vwf	ENSMUSG00000001930	-0.21	0.04	-0.3	ns	-0.03	Haemostasis

Expression profile of the 92 genes, shown to be significantly up- or downregulated in inflamed colonic mucosa of CD or UC patients [Table 1]. Data represent gene expression in colon of PAC IL-10 k.o. mice [ $n = 12$ ] compared with C57BL/6J WT mice [ $n = 3$ ], AdTr mice [ $n = 9$ ] compared with BALB/c WT mice [ $n = 5$ ] and DSS mice [ $n = 6$ ] compared with BALB/c WT mice [ $n = 7$ ]. RNA sequencing was performed on colon samples and the *p*-value was adjusted for multiple testing. Fold change values have been transformed to log<sub>2</sub>-scale [FC], thus positive FC values indicate an upregulation, whereas negative FC values indicate a downregulation in gene expression. An adjusted [Adj] *p*-value  $\leq 0.05$  was considered significant. The colon samples of the DSS mice and their BALB/c WT controls were pooled before analyses, thus the significance level could not be calculated. FC, fold change; ns, non-significant; nd, not detectable.

from UC and CD patients; 92 of these genes demonstrated a significant differential expression in either UC or CD patients compared with non-IBD controls [Table 1]. In inflamed UC mucosa, 86/115 genes [75%] were upregulated and 6/115 genes [5%] were downregulated compared with non-IBD controls. In inflamed CD mucosa, 58/115 genes [50%] were upregulated and 4/115 genes [3%] were downregulated compared with non-IBD controls; 62 genes were consistently dysregulated in both IBD subtypes, whereas 30 were unique to UC. None of the studied genes were uniquely dysregulated in CD. The 10 most dysregulated genes

by FC value in UC were *REG1A* [FC +4.66], *LCN2* [FC +4.66], *CXCL1* [FC +4.41], *NOS2* [FC +3.80], *MMP3* [FC +3.74], *S100A9* [FC +3.47], *CR2* [FC +2.96], *MMP7* [FC +2.90], *MMP9* [FC +2.81], *TIMP1* [FC +2.80], and *C3* [FC +2.80]. The 10 most dysregulated genes in CD were similarly *REG1A* [FC +4.54], *LCN2* [FC +4.12], *CXCL1* [FC +3.55], *NOS2* [FC +3.02], *MMP3* [FC +2.29] and *S100A9* [FC +2.25], *IL1B* [FC +2.52], *CXCL2* [FC +2.43], *CCL20* [FC +2.24], and *CD55* [FC +2.03]. The expression of *IL23R*, *DEFB1*, *PPARG*, and *ABCB1* was significantly decreased in both diseases [Table 1].

### 3.2. Disease manifestations of the experimental colitis models

Piroxicam-treated IL-10 k.o. mice had a significant body weight loss and increased faecal score at termination compared with age-matched IL-10 k.o. mice receiving normal chow. The colonic W:L ratio was significantly higher in PAC IL-10 k.o. mice compared with IL-10 k.o. and C57BL/6J WT mice. A tendency towards increased histology score was also observed in PAC IL-10 k.o. mice [Figure 1A]. Colonic W:L ratio and histology score did not differ between IL-10 k.o. and C57BL/6J WT mice, and they did not present any notable histopathological lesions [Figure 1A]. SCID mice reconstructed with CD4<sup>+</sup>CD25<sup>-</sup> T cells had reduced percentage weight change [ $p = 0.095$ ] and significantly increased faecal score at termination compared with SCID mice. The colonic W:L ratio was significantly higher in AdTr mice than in SCID and BALB/c WT mice [Figure 1B]. Histopathological analysis was not performed due to the well-described correlation between W:L ratio and histology score in the CD4<sup>+</sup>CD25<sup>-</sup> AdTr model.<sup>14</sup> DSS treatment of BALB/c mice resulted in significantly increased faecal score, colonic W:L ratio and histology score at termination compared with BALB/c WT mice [Figure 1C].

### 3.3. Transcriptional profiles of the experimental colitis models

Of the 92 genes which were dysregulated in CD and/or UC patients, 71 [77%] were significantly differentially expressed in the colon of PAC IL-10 k.o. mice compared with C57BL/6J WT mice [Table 2]. Eight of these genes were expressed in the opposite direction between the PAC IL-10 k.o. model and the human samples [*Il23r*, *Cx3cl1*, *Cxcl12*, *Pparg*, *Col6a3*, *Vegfc*, *C5*, and *Vwfl*]. The 10 most dysregulated genes by FC value in the colon of PAC IL-10 k.o. mice were *S100a8* [FC +6.29], *S100a9* [FC +5.92], *Nos2* [FC +5.24], *Cxcl5* [FC +5.20], *Cxcl9* [FC +4.50], *Cxcl10* [FC +4.22], *Lcn2* [FC +3.79], *Mmp7* [FC +3.74], *Mmp10* [FC +3.48], and *Il1b* [FC +3.46]. In the AdTr model, 59 out of the 92 genes [64%] were significantly differentially expressed compared with BALB/c WT mice [Table 2]. Six of these genes were expressed in the opposite direction between the AdTr model and the human samples [*Ccr6*, *Cldn1*, *Col1a2*, *Col6a3*, *Vim*, and *Cr2*]. The 10 most dysregulated genes in the AdTr model were *S100a8* [FC +7.54], *S100a9* [FC +6.92], *Nos2* [FC +6.28], *Lcn2* [FC +4.82], *Cxcl9* [FC +4.59], *Ltf* [FC +4.31], *Cxcl10* [FC +3.86], *Cxcl5* [FC +3.77], *Mmp7* [FC +3.49], and *Tnf* [FC +3.21]. A Venn diagram illustrates the distribution of genes differentially expressed in the PAC IL-10 k.o. and AdTr models [Figure 2]. Gene expression in the colon of DSS mice is listed in Table 2. Due to the pooling of mucosa samples, no statistical significance of differences could be calculated between DSS and BALB/c WT mice. However, 10 highly upregulated genes in the DSS model included *S100a8* [FC +6.11], *S100a9* [FC +5.46], *Nos2* [FC +5.29], *Cxcl9* [FC +3.83], *Cxcl13* [FC +3.74], *Cxcl5* [FC +3.70], *Cxcl1* [FC +3.53], *Il1b* [FC +3.36], *Cxcl10*, and *Mmp3* [FC +3.11].

Figure 3 shows correlations between expression level of the six genes which were found to be most highly dysregulated in UC and CD patients, and colonic W:L ratio in PAC IL-10 k.o. and AdTr mice. A significant correlation was observed between all gene expression levels and W:L ratio of individual PAC IL-10 k.o. mice, except *Reg1*. The expression levels of *Lcn2*, *Nos2*, and *S100a9* correlated significantly with W:L ratio of individual AdTr mice as well [Figure 3]. Additionally, *S100a8* expression was significantly correlated with W:L ratio both in the PAC IL-10 k.o. and AdTr models [ $r_s = 0.83$ ,  $p = 0.0016$ , and  $r_s = 0.80$ ,  $p = 0.0138$ , respectively].

### 3.4. Gene expression across the colitis models

The expression pattern of each gene, standardised across all mice, is shown in heat maps [Figures 4–6]. PAC IL-10 k.o. and AdTr mice are organised according to the degree of colitis, represented by the colonic W:L ratio. In general, the heat maps showed an overexpression of cytokine, cytokine receptor, intracellular signaling, and cell surface marker genes in PAC IL-10 k.o. mice, and the gene expression levels seemed to be associated with the degree of colitis [Figure 4]. This expression profile observed in the PAC IL-10 k.o. model seemed less pronounced in AdTr and DSS mice, and only few transcripts were associated with the degree of colitis in AdTr mice [Figure 4]. In general, chemokine, chemokine receptors, and adhesion molecule genes were overexpressed in PAC IL-10 k.o., AdTr, and DSS mice [Figure 5]. In addition, PAC IL-10 k.o. mice had an overexpression of tissue remodelling genes, and AdTr mice showed a high expression of most bacterial sensing genes [Figure 6]. No notable differences in gene expression were observed between IL-10 k.o. mice and C57BL/6J WT mice, except for the intracellular signaling genes, *Stat3*, *Stat5a*, and *Jak2*, which seemed to be overexpressed in IL-10 k.o. mice [Figure 4]. SCID mice had a low expression of all genes, with the exception of *Abcb1a*, *Casp1*, and *Isg15* [Figure 6].

### 3.5. Gene expression patterns related to T helper cells.

Several genes associated with a Th1, Th2, and Th17 response<sup>7,28</sup> were significantly overexpressed in inflamed mucosa of both CD and UC patients compared with non-IBD controls [Table 1]. The expression of Th1-associated genes was also significantly upregulated in the colon of PAC IL-10 k.o. and AdTr mice compared with C57BL/6J and BALB/c WT mice, respectively, including *Ifng* [FC +2.20/ +1.30], *Il12b* [FC +0.81/ +0.35], *Stat1* [FC +2.57/ +2.36], *Tbx21* [FC +0.64/ +0.69], *Cxcr3* [FC +0.84/ +1.0], and *Cxcl10* [FC +1.73/ +2.55]. These genes also seemed upregulated in the DSS model compared with BALB/c WT controls [FC +0.90, +0.23, +2.49, +1.45, +1.08, and +3.11, respectively] [Table 2]. Th2-associated chemokine and transcription factor genes, including *Gata3* [FC +0.67/ +0.50/ +1.27] and *Ccl11* [eotaxin-1] [FC +0.83/ +1.0/ +0.97], were dysregulated in the PAC IL-10 k.o., AdTr, and DSS models, whereas *Ccl17* [TARC] was upregulated only in the AdTr model [FC +1.21]. The expression of the Th17-associated genes *Il17a* [FC +1.05/ +0.29], *Il17f* [FC +0.63/ +0.24], *Il22* [FC +1.08/ +0.34] and *Stat3* [FC +0.57/ +0.32] was significantly upregulated in the PAC IL-10 k.o. and AdTr colitis models, whereas the expression of *Ccr6* was significantly downregulated only in the AdTr model [FC -0.59]. Particularly *Stat3* and *Ccr6* seemed overexpressed in the DSS model [FC +0.76 and +2.52, respectively]. A significantly differential expression of *Il21* was detected in the PAC IL-10 k.o. model [FC +0.19] whereas no dysregulation was observed in *Il23a* in any of the experimental models [Table 2].

## 4. Discussion

A detailed knowledge about the applied animal models, as well as the corresponding human disease, is necessary for proper interpretation of data achieved in preclinical *in vivo* experiments. In this study, RNAseq analyses were performed on inflamed colon samples from IBD patients and three mouse models of colitis to examine and compare the multiple pathophysiological processes involved in the different settings. To our knowledge, this is the first study to reveal the expression pattern of numerous IBD-associated genes in the PAC



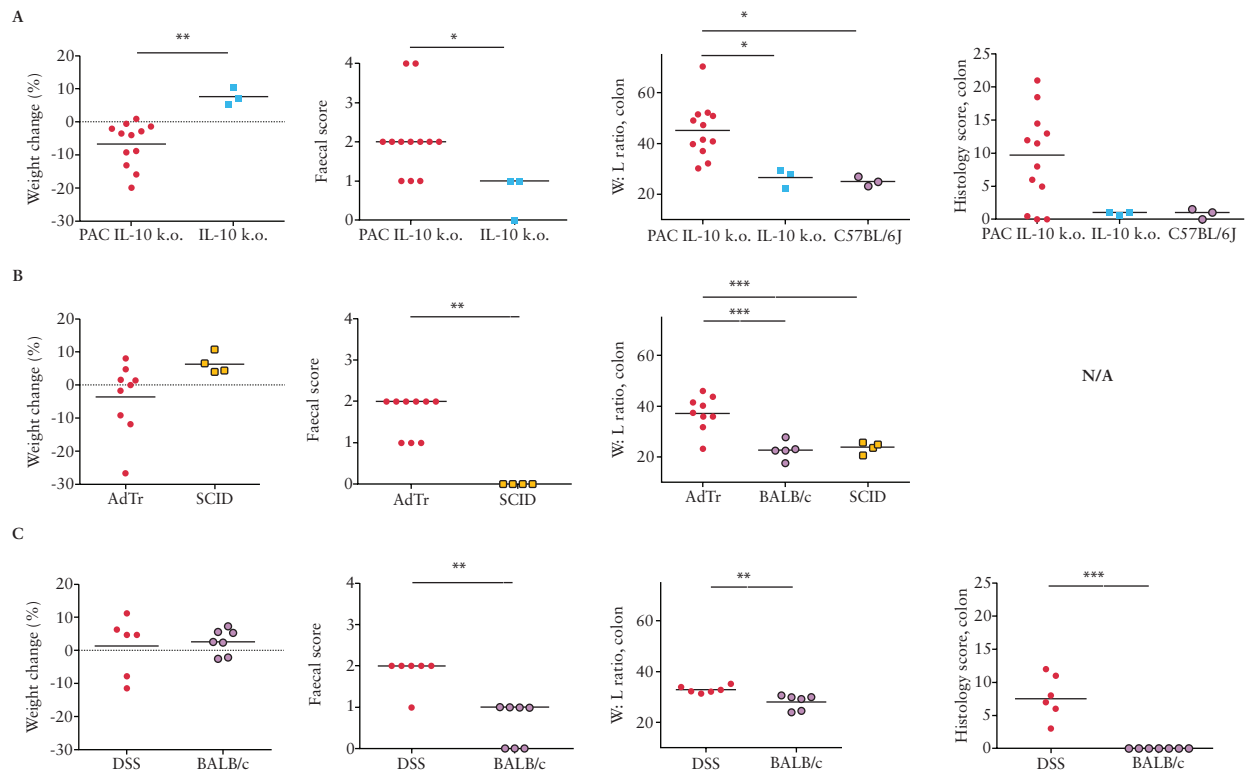


**Figure 1.** Disease manifestations of the experimental colitis models. Presence of colitis in the mice was confirmed by the assessment of percentage body weight change from Day 0 [mean], faecal score [median], colonic W:L ratio [mg/cm] [mean] and histological score [median] at termination. [A] IL-10 k.o. mice were fed piroxicam in the chow from Day 0 until termination at Day 10 [PAC IL-10 k.o.]. IL-10 k.o. mice fed normal chow or C57BL/6J wild-type [WT] mice were used as controls. [B] Splenic CD4<sup>+</sup>CD25<sup>+</sup> T cells were transferred from BALB/c to SCID mice at Day 0 [AdTr]. The mice were terminated between Days 28–37. BALB/c WT or SCID mice were used as controls. [C] BALB/c mice received DSS in the water from Day 0 until Day 5. From day 5 until termination, Day 8, the mice received water without DSS [DSS]. BALB/c WT mice were used as controls. Student's t test or one-way ANOVA with Holm-Sidak's multiple comparison test was used for the comparison of parametric data. Mann-Whitney test or Kruskal-Wallis with Dunn's multiple comparison tests were used for the comparison of non-parametric data. W: L, weight:length; N/A, not available.

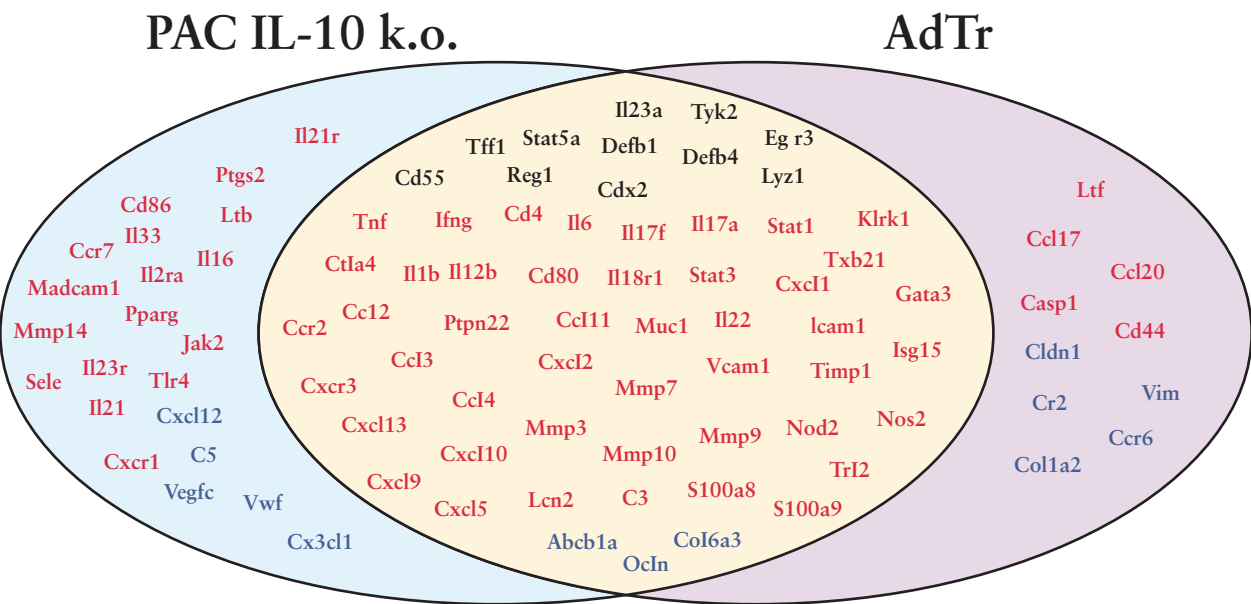


**Figure 2.** Venn diagram illustrating the distribution of significantly up- [red] or downregulated [blue] genes in colon tissue of the PAC IL-10 k.o. and AdTr models compared with their respective wild-type controls. Black marking denotes non-significantly dysregulated genes.

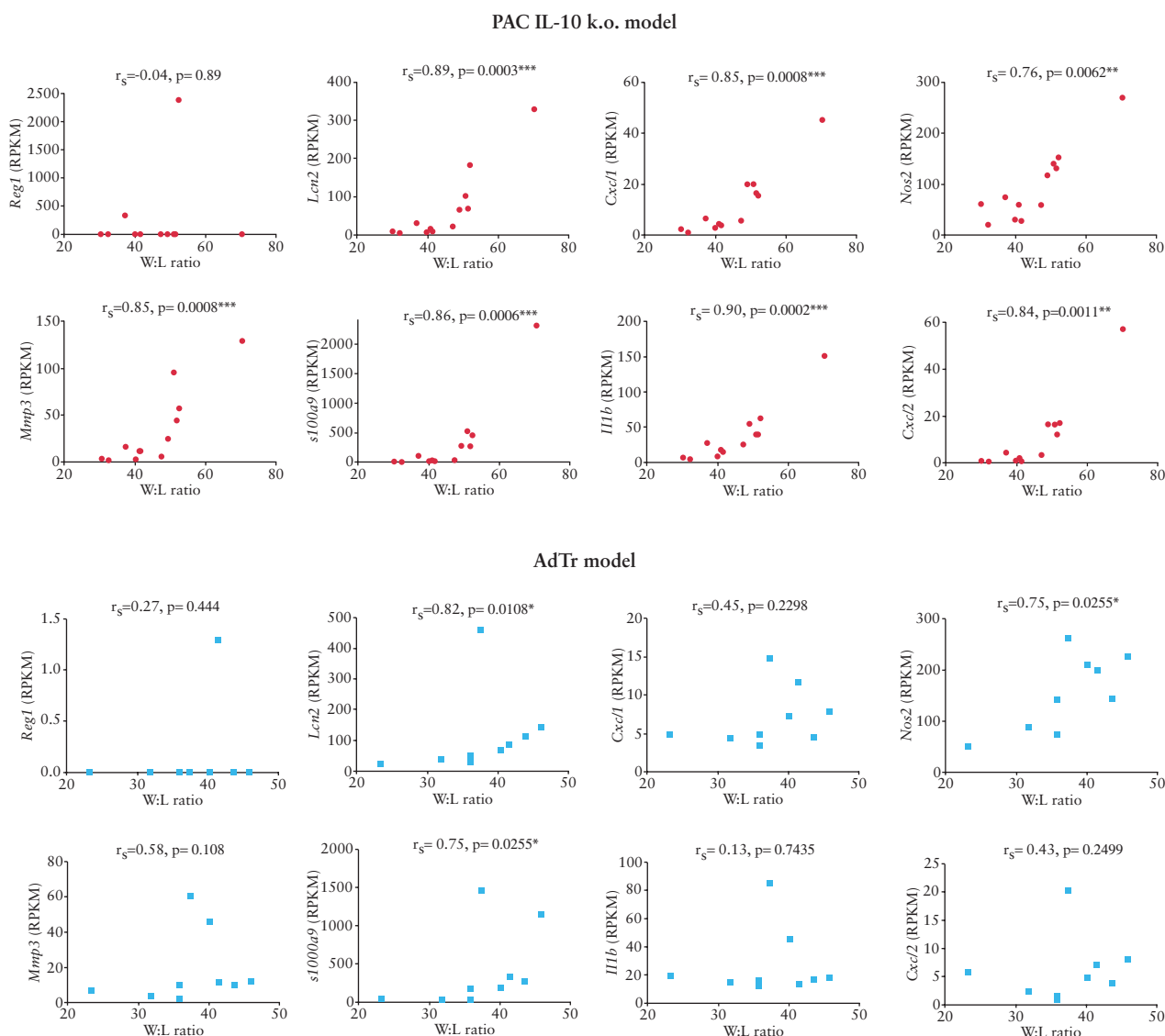


**Figure 3.** Correlation between gene expression levels and colonic weight:length [W:L] ratio of individual PAC IL-10 k.o. mice and AdTr mice. The included genes are the six most dysregulated genes in UC and CD patients. Four genes have a common high expression in both diseases [*Reg1*, *Lcn2*, *Cxcl1*, and *Nos2*]. RPKM, reads per kilobase of transcript per million reads.

IL-10 k.o. model. The main difference between our study and previous key publications comparing transcriptional changes in experimental colitis models is the preselection of genes to be studied.<sup>60,61,62</sup> We only included those genes which we ourselves confirmed to be differentially expressed in CD and/or UC patients using deep sequencing. We believe that this approach enabled a more detailed and qualified transcriptional profiling of relevant mouse models. Even though our selection of colonic transcripts omitted important pathogenic pathways, such as the  $\alpha_4\beta_7$  integrin, this paper provides expanded information about the pathways underlying experimental colitis and a knowledge-based platform for future preclinical research.

In general, the gene expression profiles indicated shared pathogenic pathways and protective biological mechanisms secondary to ongoing colitis. We found that some of the most upregulated genes in inflamed colonic CD and UC mucosa were involved in anti-bacterial pathways, including *Reg1A*, *LCN2*, *NOS2*, and *S100A9*. A high expression of *Lcn2*, *Nos2*, *S100a9*, and *S100a8* was also revealed in

the colon of the three colitis models, and the expression levels correlated with the macroscopic parameter of colitis, i.e. colonic W:L ratio, in both the PAC IL-10 k.o. and the AdTr model. Lipocalin 2 [*Lcn2*], inducible nitric oxide synthase [iNOS] and S100A8/S100A9 protein complex [calprotectin] are components of the innate immune response. Calprotectin is abundantly expressed in the cytosol of myeloid cells and secreted by activated phagocytes, especially neutrophils.<sup>63,64</sup> Calprotectin is a well-recognised marker for monitoring disease activity in IBD patients.<sup>65,66</sup> Likewise, faecal *Lcn2* levels positively correlate with intestinal inflammatory activity in both humans and mice<sup>67,68</sup> and is suggested to be a sensitive non-invasive diagnostic marker. *Lcn2* protein is abundant in neutrophil granules and pro-inflammatory stimuli, like Toll-like receptor 3 signaling and IL-1 $\beta$  stimulation induce its release by colonic epithelial cells.<sup>69</sup> Through the binding of bacterial siderophores, *Lcn2* has bacteriostatic effect and may play a role in dysbiosis, a key characteristic of IBD. Despite their highly dynamic regulation and clear association with colitis, the extent to which calprotectin and *Lcn2* drive or suppress gut

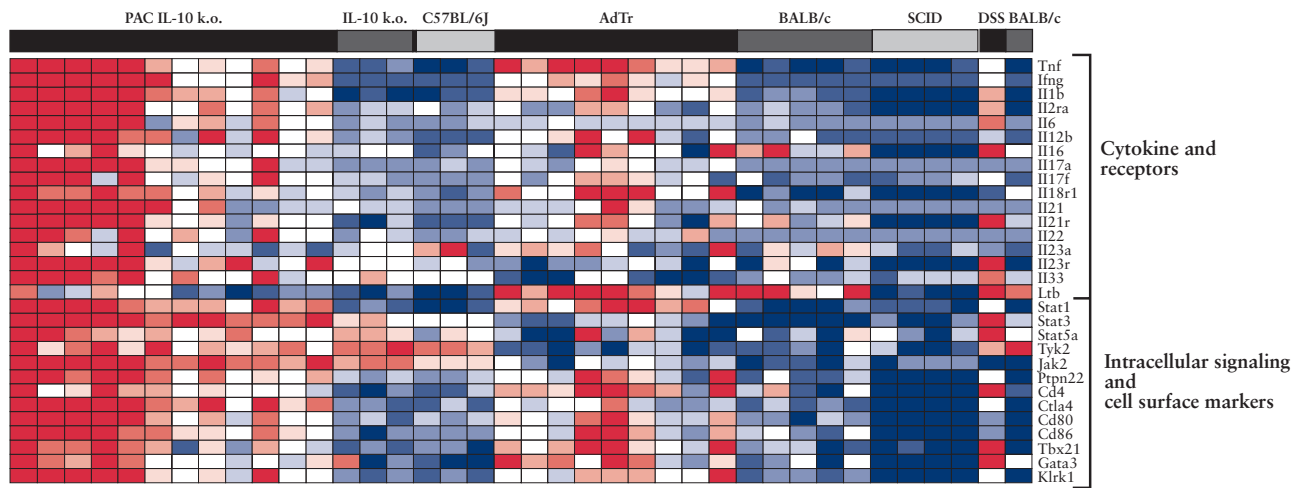


**Figure 4.** Heat map presentation of RNAseq expression for IBD-associated genes related to cytokine, cytokine receptor, intracellular signaling, and cell surface markers in the colon of experimental colitis models. Each row represents expression of one gene standardised across all mice. Each column represents the sample from one individual mouse, except in the DSS and BALB/c control mice, in which colon tissue was pooled before analysis. High gene expression levels are marked red, low expression levels are marked blue, and neutral expression levels are marked white.

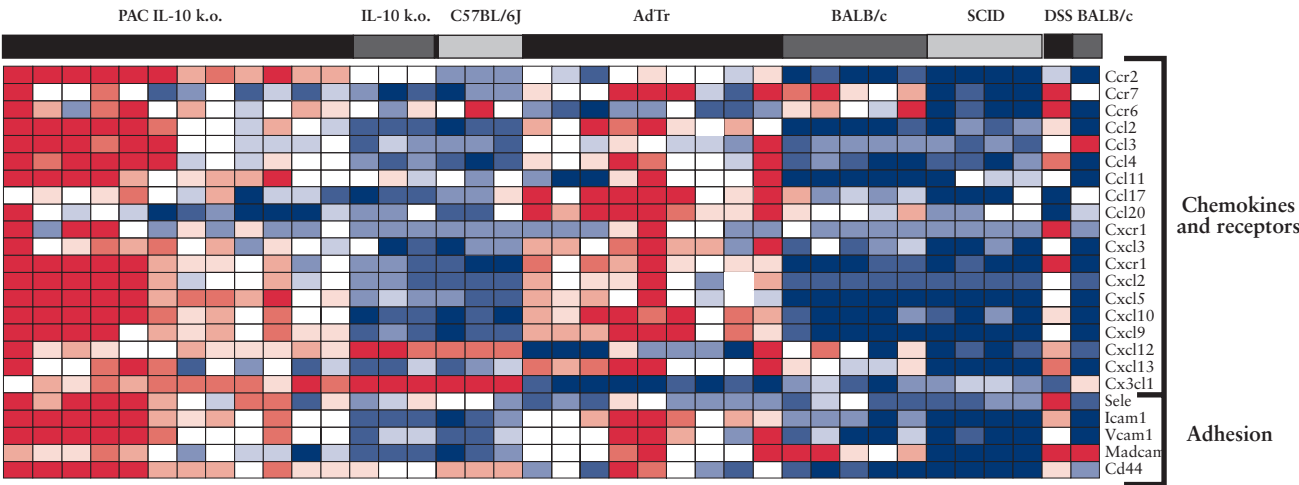


**Figure 5.** Heat map presentation of RNAseq expression for IBD-associated genes related to chemokine, chemokine receptor, and adhesion molecules in the colon of experimental colitis models. Each row represents expression of one gene standardised across all mice. Each column represents the sample from one individual mouse, except for the DSS and BALB/c control mice, in which colon tissue was pooled before analysis. High gene expression levels are marked red, low expression levels are marked blue, and neutral expression levels are marked white.

inflammation is still not clarified. *Nos2* encodes iNOS that synthesises the free radical nitric oxide [NO]. NO is a ubiquitous molecule with multiple biological functions in the gut mucosa, depending on concentration and duration, including DNA damage, cytostatic effects, and apoptosis.<sup>70,71,72</sup> A *NOS2* gene variant has been associated with early-onset IBD and increased iNOS activity, contributing to nitrosative stress and peroxynitrite-mediated tissue damage in the intestine.<sup>73</sup> In experimental colitis models, the effects of iNOS genetic ablation are contradictory. Knocking out the iNOS encoding gene had no effect on spontaneously developed chronic colitis in IL-10 k.o. mice,<sup>74</sup> whereas iNOS deficiency significantly attenuated disease in acute DSS-induced colitis.<sup>75</sup> The discrepancy is attributed to the different pathophysiology of the models and it indicates that iNOS contributes mainly during acute colitis. Depletion studies are necessary to further assess the impact of iNOS, as well as S100A8/S100A9 and Lcn2, in the pathogenesis of PAC IL-10 k.o. mice.

As previously described,<sup>43</sup> numerous chemokine and endothelial adhesion molecule genes were overexpressed in the inflamed mucosa of both UC and CD patients, orchestrating the recruitment of leukocytes into the tissue. *Cxcl5* and *Cxcl9-10* were highly upregulated in the colon of all three colitis models, and the expression levels of *Cxcl1-2* were significantly correlated with W:L ratio in PAC IL-10 k.o. mice. CXCL1-2 and CXCL5 are implicated in recruitment of chemokine receptor expressing CXCR2<sup>+</sup> neutrophils,<sup>76</sup> whereas CXCL9-10 attract CXCR3<sup>+</sup> lymphocytes, preferentially Th1.<sup>77</sup> The expression of Th1- as well as Th17-associated cytokine genes was upregulated in the models, particularly in PAC IL-10 k.o. mice. Moreover, *Ccl2* and *Ccr2*, which mediate migration and activation of monocytes and macrophages,<sup>77,78</sup> were overexpressed in the experimental colitis models. This is supported by the observed upregulation of proinflammatory cytokine genes, like *Tnf*, *Il1b*, and *Il6* in the colonic mucosa and an increased expression of the

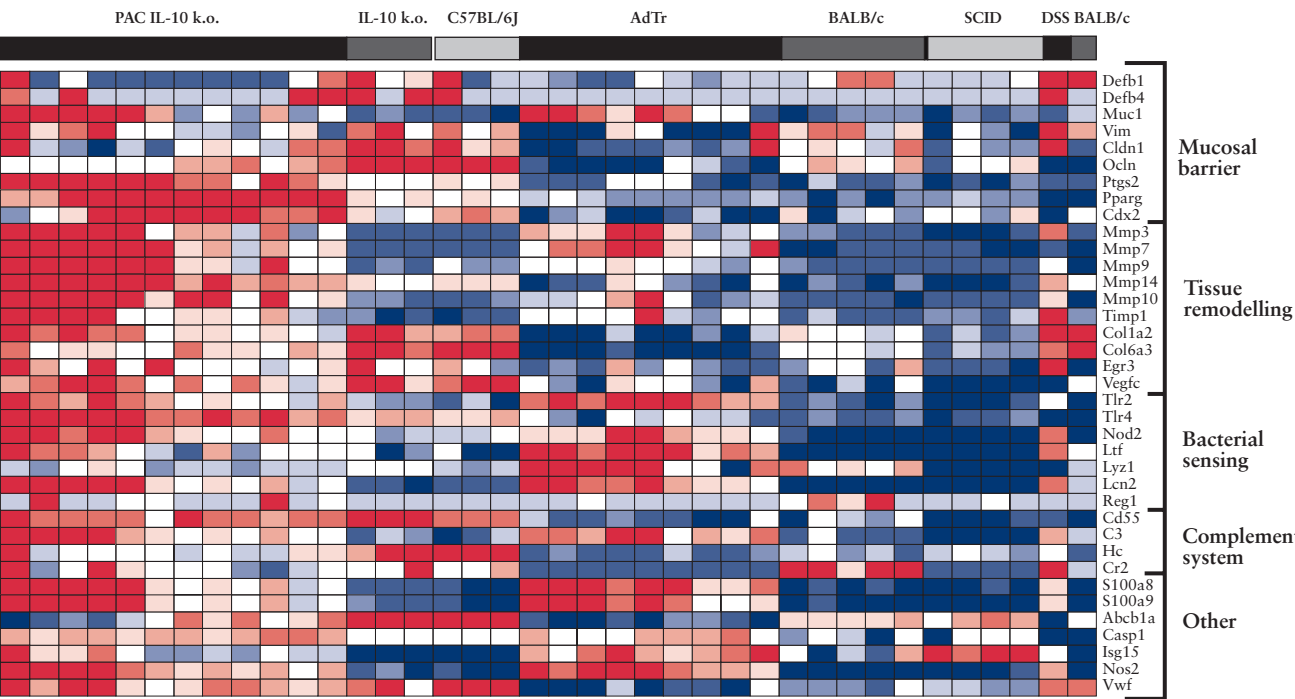


**Figure 6.** Heat map presentation of RNAseq expression for IBD-associated genes related to mucosal barrier, tissue remodelling, bacterial sensing, complement system and others in the colon of experimental colitis models. Each row represents expression of one gene standardised across all mice. Each column represents the sample from one individual mouse, except in the DSS and BALB/c control mice, in which colon tissue was pooled before analysis. High gene expression levels are marked red, low expression levels are marked blue, and neutral expression levels are marked white.

pattern-recognition receptor genes involved in bacterial sensing and clearance by macrophages.<sup>79</sup>

The genetic background influences the expression profiles in mice, although the effect is rather limited compared with disease-related changes.<sup>80</sup> Thus, the models were compared with WT mice of the same inbred strain, but we also performed gene expression profiling which was standardised across all included mouse strains and presented in heat maps. In the heat maps, inflammation-related genes seemed to be associated with colonic W:L ratio in PAC IL-10 k.o. mice, but this was less pronounced in AdTr mice. Previously, the W:L ratio has been described to be significantly associated with the histology score of individual AdTr mice [ $r$  0.91,  $p$  < 0.001].<sup>14</sup> However, in our study the AdTr mice were randomly sacrificed at different time points after chronic colitis was established [Days 28–37 after cell transfer<sup>14</sup>], which may influence the variation between mice, as well as the correlation to the inflammatory expression profile. The heat maps revealed a pronounced overexpression of matrix metalloproteinases [MMPs] and the inhibitor [TIMP1] encoding genes in PAC IL-10 k.o. mice. This was confirmed by significantly increased fold changes in all analysed MMPs genes in the PAC IL-10 k.o. model compared with C57BL/6J WT controls, and a significant correlation between *Mmp3* expression level and W:L ratio in the model. MMPs and *TIMP1* gene expression was upregulated in inflamed IBD mucosa but tended to be higher in UC than CD, in accordance with previously published data<sup>23,53</sup>. In IBD patients, MMP1-3, MMP14, and *TIMP1* mRNA expression has shown significant correlation with the histological degree of acute inflammation, and the highest expressions were observed in ulcerated tissue.<sup>53</sup> The PAC IL-10 k.o. and AdTr models develop histological lesions which resemble the pathology of CD.<sup>14,15,17,81</sup> The histological changes are characterised by extensive infiltration of immune cells and epithelial hyperplasia.

Focal transmural inflammation and ulcerations are observed in severe cases. The DSS model is more haemorrhagic; it develops histological lesions characterised by crypt distortion, cell infiltration, and mucosal erosions.<sup>12,13</sup> Thus, the observed overexpression of MMPs is most likely related to extensive leukocyte infiltration<sup>82</sup> but also to ulcerations and wound healing, particularly in UC patients and DSS mice in which ulcerations are predominant.

Interpretation of the heat maps and RNAseq analyses should be done with cautious. Regional differences in transcriptional pattern along the colon have been observed under normal<sup>26</sup> and inflamed<sup>82</sup> conditions. In the mouse models, colon samples were collected at different anatomical locations, i.e. at the site most severely affected.<sup>12,14,17</sup> The degree of colonic hyperplasia in the various models may mask transcriptional differences and, in contrast to IBD patients, a full-thickness colon section was used for analysis. This increases the heterogeneity of cell types in the samples and hampers the comparison of gene expression patterns between IBD and experimental colitis. Moreover, transcripts differentially expressed in the deeper mucosal layers of IBD patients were not evaluated, which is misleading, particularly in transmural CD lesions.

The PAC IL-10 k.o. model had a higher number of significantly dysregulated IBD-associated genes than the AdTr model, primarily as a result of more upregulated cytokine and cytokine receptor genes. Previously, the expression pattern of 32 genes in a CD4<sup>+</sup>CD45RB<sup>high</sup> AdTr model was shown to most closely reflect the altered transcriptional profile of human IBD patients compared with chemically-induced colitis models.<sup>62</sup> In contrast to our study, SCID mice were used as controls for the AdTr model. SCID mice are immunodeficient and have low basis expression of inflammatory genes. Thus, they probably enable detection of more significant transcriptional changes than a WT control. Nevertheless, since early bacterial



colonisation influences the immune reactivity later in life,<sup>83,84</sup> our use of non-littermate WT mice as controls could have misled the inflammatory expression profile in both the AdTr and PAC IL-10 k.o. models. Still, a clear overlap in the gene expression levels of healthy IL-10 k.o. mice and non-littermate WT mice was observed in the heat maps. Few genes, like *Stat3*, *Stat5a*, and *Jak2*, were over-expressed in IL-10 k.o. mice compared with WT mice. Since IL-10 k.o. mice did not present any lesions in the colon, these intracellular signaling transcripts were not specifically associated with an inflammatory phenotype and are probably not pivotal drivers of colitis in the PAC IL-10 k.o. mice. In another study, only few IBD-associated genes were differentially expressed in C57BL/6J IL-10 k.o. mice compared with non-littermate WT mice, but the number increased markedly when colitis was induced by inoculation of *Enterococcus* species.<sup>60</sup> This again demonstrates that many transcriptional pathways in colitis models are dysregulated due to inflammatory processes. The pathophysiology of PAC IL-10 k.o. mice combines the lack of IL-10, a crucial immunoregulatory cytokine,<sup>85</sup> with reduced mucosal barrier integrity. Piroxicam treatment suppresses the production of prostaglandins in the colon<sup>86</sup> and subsequently increases mucosal permeability and translocation of luminal bacteria.<sup>87</sup> A pivotal role for barrier disturbance in the pathogenesis of colitis was supported by the observed up- or downregulation of crucial mucosal barrier-associated genes in our study. Such a 'multihit' model, with additive abnormalities in several homeostatic pathways, promotes proinflammatory conditions and is suggested in IBD pathogenesis.<sup>88</sup>

In summary, IBD patients and experimental colitis models share many similarities in their transcriptional profiles, probably as a consequence of unspecific inflammation. However, gene expression did vary among colitis models due to differences in model design, e.g. the DSS model appears appropriate in studying the aspects of mucosal healing and the PAC IL-10 k.o. model could indeed be useful in the preclinical screening of biologicals with anti-cytokine activity. However, IBD is a heterogeneous disease and *in vivo* models should therefore complement, not substitute, each other in preclinical research and drug screening. In conclusion, the PAC IL-10 k.o. model was confirmed as a valuable mouse model of colitis. It most closely reflected the altered expression profile of IBD patients and thus mimicked numerous molecular pathways underlying IBD, some of which could be used as biomarkers of disease activity.

## Supplementary Data

Supplementary data are available at *ECCOJC* online.

## Conflicts of interest

The authors declare no conflicts of interests.

## Acknowledgments

This work was supported by the Novo Nordisk—LIFE *In Vivo* Pharmacology Centre [LIFEPHARM], the Department of Immunopharmacology, Novo Nordisk A/S and NNRC—Molecular Immunology, Novo Nordisk A/S. All sponsors contributed to study design, collection, analysis, and interpretation of data, in writing the report, and agreed to submit the paper for publication.

The authors would like to thank Claus Haase, Director of Department of Immunopharmacology, Novo Nordisk, for general support and revision of the manuscript, and Wenfeng Xu, Director of NNRC—Molecular Immunology, Novo Nordisk, for general support. Also, the authors thank Lotte Friis Wilson, Camilla Frost Sørensen, and Anders Kajhøj Hansen for excellent technical assistance and the Laboratory Animal Science group at Novo Nordisk, Maaloev, for assistance with mouse husbandry.

All authors contributed significantly to the work of the article. KH conceived and planned the study, interpreted the data and wrote the paper. TLH conceived the study, acquired the animal samples, interpreted the data and helped to draft the paper. BK, BF, and KS analysed and interpreted the data and performed the statistical analyses. JL acquired the human data and samples. AKH contributed to conceiving the study and interpreting the data. All authors reviewed the manuscript and approved the final version. Writing assistance was not obtained.

## References

1. Cho JH, Gregersen PK. Genomics and the multifactorial nature of human autoimmune disease. *N Engl J Med* 2011;**365**:1612–23.
2. Franke A, McGovern DP, Barrett JC, et al. Genome-wide meta-analysis increases to 71 the number of confirmed Crohn's disease susceptibility loci. *Nat Genet* 2010;**42**:1118–25.
3. Jostins L, Ripke S, Weersma RK, et al. Host-microbe interactions have shaped the genetic architecture of inflammatory bowel disease. *Nature* 2012;**491**:119–24.
4. Anderson CA, Boucher G, Lees CW, et al. Meta-analysis identifies 29 additional ulcerative colitis risk loci, increasing the number of confirmed associations to 47. *Nat Genet* 2011;**43**:246–52.
5. Shih DQ, Targan SR. Insights into IBD pathogenesis. *Curr Gastroenterol Rep* 2009;**11**:473–80.
6. Dieckgraefe BK, Stenson WF, Korzenik JR, Swanson PE, Harrington CA. Analysis of mucosal gene expression in inflammatory bowel disease by parallel oligonucleotide arrays. *Physiol Genomics* 2000;**4**:1–11.
7. Granlund A, Flatberg A, Ostvik AE, et al. Whole genome gene expression meta-analysis of inflammatory bowel disease colon mucosa demonstrates lack of major differences between Crohn's disease and ulcerative colitis. *PLoS One* 2013;**8**:e56818.
8. Ordas I, Eckmann L, Talamini M, Baumgart DC, Sandborn WJ. Ulcerative colitis. *Lancet* 2012;**380**:1606–19.
9. Baumgart DC, Sandborn WJ. Crohn's disease. *Lancet* 2012;**380**:1590–605.
10. Baumgart DC, Sandborn WJ. Inflammatory bowel disease: clinical aspects and established and evolving therapies. *Lancet* 2007;**369**:1641–57.
11. Solomon L, Mansor S, Mallon P, et al. The dextran sulphate sodium [DSS] model of colitis: an overview. *Comp Clin Pathol* 2010;**19**:235–9.
12. Okayasu I, Hatakeyama S, Yamada M, Ohkusa T, Inagaki Y, Nakaya R. A novel method in the induction of reliable experimental acute and chronic ulcerative colitis in mice. *Gastroenterology* 1990;**98**:694–702.
13. Cooper HS, Murthy SN, Shah RS, Sedergran DJ. Clinicopathologic study of dextran sulfate sodium experimental murine colitis. *Lab Invest* 1993;**69**:238–49.
14. Kjellev S, Lundsgaard D, Poulsen SS, Markholst H. Reconstitution of Scid mice with CD4+CD25– T cells leads to rapid colitis: An improved model for pharmacologic testing. *Int Immunopharmacol* 2006;**6**:1341–54.
15. Morrissey PJ, Charrier K, Braddy S, Liggitt D, Watson JD. CD4+ T cells that express high levels of CD45RB induce wasting disease when transferred into congenic severe combined immunodeficient mice. Disease development is prevented by cotransfer of purified CD4+ T cells. *J Exp Med* 1993;**178**:237–44.
16. Powrie F, Leach MW, Mauze S, Caddle LB, Coffman RL. Phenotypically distinct subsets of CD4+ T cells induce or protect from chronic intestinal inflammation in C. B-17 scid mice. *Int Immunol* 1993;**5**:1461–71.
17. Holgersen K, Kvist PH, Markholst H, Hansen AK, Holm TL. Characterisation of enterocolitis in the piroxicam-accelerated interleukin-10 knock out mouse: A model mimicking inflammatory bowel disease. *J Crohns Colitis* 2013;**8**:147–60.
18. Holgersen K, Kvist PH, Hansen AK, Holm TL. Predictive validity and immune cell involvement in the pathogenesis of piroxicam-accelerated colitis in interleukin-10 knockout mice. *Int Immunopharmacol* 2014;**21**:137–47.
19. Nicklas W, Baneux P, Boot R, et al. Recommendations for the health monitoring of rodent and rabbit colonies in breeding and experimental units. *Lab Anim* 2002;**36**:20–42.

20. Woywodt A, Ludwig D, Neustock P, *et al.* Mucosal cytokine expression, cellular markers and adhesion molecules in inflammatory bowel disease. *Eur J Gastroenterol Hepatol* 1999;11:267–76.
21. Niessner M, Volk BA. Altered Th1/Th2 cytokine profiles in the intestinal mucosa of patients with inflammatory bowel disease as assessed by quantitative reversed transcribed polymerase chain reaction [RT-PCR]. *Clin Exp Immunol* 1995;101:428–35.
22. Scarpa M, Behboo R, Angriman I, *et al.* The role of costimulatory molecules CD80 and CD86 and IFN $\gamma$  in the pathogenesis of ulcerative colitis. *Dig Dis Sci* 2004;49:1738–44.
23. Lawrance IC, Fiocchi C, Chakravarti S. Ulcerative colitis and Crohn's disease: distinctive gene expression profiles and novel susceptibility candidate genes. *Hum Mol Genet* 2001;10:445–56.
24. Planell N, Lozano JJ, Mora-Buch R, *et al.* Transcriptional analysis of the intestinal mucosa of patients with ulcerative colitis in remission reveals lasting epithelial cell alterations. *Gut* 2013;62:967–76.
25. Stevens C, Walz G, Singaram C, *et al.* Tumor necrosis factor- $\alpha$ , interleukin-1  $\beta$ , and interleukin-6 expression in inflammatory bowel disease. *Digest Dis Sci* 1992;37:818–26.
26. Noble CL, Abbas AR, Cornelius J, *et al.* Regional variation in gene expression in the healthy colon is dysregulated in ulcerative colitis. *Gut* 2008;57:1398–405.
27. Noble CL, Abbas AR, Lees CW, *et al.* Characterization of intestinal gene expression profiles in Crohn's disease by genome-wide microarray analysis. *Inflamm Bowel Dis* 2010;16:1717–28.
28. Christophi GP, Rong R, Holtzapple PG, Massa PT, Landas SK. Immune markers and differential signaling networks in ulcerative colitis and Crohn's disease. *Inflamm Bowel Dis* 2012;18:2342–56.
29. Seegert D, Rosenstiel P, Pfahler H, Pfefferkorn P, Nikolaus S, Schreiber S. Increased expression of IL-16 in inflammatory bowel disease. *Gut* 2001;48:326–32.
30. Autschbach F, Funke B, Katzenmeier M, Gassler N. Expression of chemokine receptors in normal and inflamed human intestine, tonsil, and liver: an immunohistochemical analysis with new monoclonal antibodies from the 8th International Workshop and Conference on human leucocyte differentiation antigens. *Cell Immunol* 2005;236:110–14.
31. Tornehave D, Zahn S, Matthiesen F, Krogh BO, Lundsgaard D. IL-21 and IL-21 receptor expression in the intestine from patients with Crohn's disease. In: Poster presentations: *Basic Science*, European Crohn's and Colitis Organisation, Feb14–16, 2013; Vienna.
32. Andoh A, Zhang Z, Inatomi O, *et al.* Interleukin-22, a member of the IL-10 subfamily, induces inflammatory responses in colonic subepithelial myofibroblasts. *Gastroenterology* 2005;129:969–84.
33. Song L, Zhou R, Huang S, *et al.* High intestinal and systemic levels of interleukin-23/T-helper 17 pathway in Chinese patients with inflammatory bowel disease. *Mediators Inflamm* 2013;2013:425915.
34. Seidelin JB, Coskun M, Kvist PH, Holm TL, Holgersen K, Nielsen OH. IL-33 promotes GATA-3 polarization of gut-derived T cells in experimental and ulcerative colitis. *J Gastroenterol* 2015;50:180–90.
35. Spalinger MR, Lang S, Weber A, *et al.* Loss of protein tyrosine phosphatase nonreceptor type 22 regulates interferon- $\gamma$ -induced signaling in human monocytes. *Gastroenterology* 2013;144:978–88.
36. Mariani P, Bachetoni A, D'Alessandro M, Lomanto D, Mazzocchi P, Speranza V. Effector Th-1 cells with cytotoxic function in the intestinal lamina propria of patients with Crohn's disease. *Dig Dis Sci* 2000;45:2029–35.
37. Roman LI, Manzano L, De La Hera A, Abreu L, Rossi I, Alvarez-Mon M. Expanded CD4 $^{+}$ CD45RO $^{+}$  phenotype and defective proliferative response in T lymphocytes from patients with Crohn's disease. *Gastroenterology* 1996;110:1008–19.
38. Chen Z, Brant SR, Li C, *et al.* CTLA4 -1661A/G and 3'UTR long repeat polymorphisms are associated with ulcerative colitis and influence CTLA4 mRNA and protein expression. *Genes Immun* 2010;11:573–83.
39. Repnik K, Potocnik U. CTLA4 CT60 single-nucleotide polymorphism is associated with Slovenian inflammatory bowel disease patients and regulates expression of CTLA4 isoforms. *DNA Cell Biol* 2010;29:603–10.
40. Scarpa M, Bortolami M, Cecchetto A, *et al.* Mucosal immune environment in colonic carcinogenesis: CD80 up-regulation in colonic dysplasia in ulcerative colitis. *Eur J Cancer* 2011;47:611–19.
41. Allez M, Tieng V, Nakazawa A, *et al.* CD4 $^{+}$ NKG2D $^{+}$  T Cells in Crohn's disease mediate inflammatory and cytotoxic responses through MICA interactions. *Gastroenterology* 2007;132:2346–58.
42. Connor SJ, Paraskevopoulos N, Newman R, *et al.* CCR2 expressing CD4 $^{+}$  T lymphocytes are preferentially recruited to the ileum in Crohn's disease. *Gut* 2004;53:1287–94.
43. Arijis I, De HG, Machiels K, *et al.* Mucosal gene expression of cell adhesion molecules, chemokines, and chemokine receptors in patients with inflammatory bowel disease before and after infliximab treatment. *Am J Gastroenterol* 2011;106:748–61.
44. Uguccioni M, Gionchetti P, Robbiani DF, *et al.* Increased expression of IP-10, IL-8, MCP-1, and MCP-3 in ulcerative colitis. *Am J Pathol* 1999;155:331–6.
45. Banks C, Bateman A, Payne R, Johnson P, Sheron N. Chemokine expression in IBD. Mucosal chemokine expression is unselectively increased in both ulcerative colitis and Crohn's disease. *J Pathol* 2003;199:28–35.
46. Puleston J, Cooper M, Murch S, *et al.* A distinct subset of chemokines dominates the mucosal chemokine response in inflammatory bowel disease. *Aliment Pharmacol Ther* 2005;21:109–20.
47. Labbe C, Boucher G, Foisy S, *et al.* Genome-wide expression profiling implicates a MAST3-regulated gene set in colonic mucosal inflammation of ulcerative colitis patients. *Inflamm Bowel Dis* 2012;18:1072–80.
48. Arijis I, De HG, Lemaire K, *et al.* Mucosal gene expression of antimicrobial peptides in inflammatory bowel disease before and after first infliximab treatment. *PLoS One* 2009;4:e7984.
49. Weber CR, Nalle SC, Tretiakova M, Rubin DT, Turner JR. Claudin-1 and claudin-2 expression is elevated in inflammatory bowel disease and may contribute to early neoplastic transformation. *Lab Invest* 2008;88:1110–20.
50. Gassler N, Rohr C, Schneider A, *et al.* Inflammatory bowel disease is associated with changes of enterocytic junctions. *Am J Physiol Gastrointest Liver Physiol* 2001;281:G216–28.
51. Coskun M, Troelsen JT, Nielsen OH. The role of CDX2 in intestinal homeostasis and inflammation. *Biochim Biophys Acta* 2011;1812:283–9.
52. de Bruyn M, Machiels K, Vandooren J, *et al.* Infliximab restores the dysfunctional matrix remodeling protein and growth factor gene expression in patients with inflammatory bowel disease. *Inflamm Bowel Dis* 2014;20:339–52.
53. von Lampe B, Barthel B, Coupland SE, Riecken EO, Rosewicz S. Differential expression of matrix metalloproteinases and their tissue inhibitors in colon mucosa of patients with inflammatory bowel disease. *Gut* 2000;47:63–73.
54. Rath T, Roderfeld M, Graf J, *et al.* Enhanced expression of MMP-7 and MMP-13 in inflammatory bowel disease: a precancerous potential? *Inflamm Bowel Dis* 2006;12:1025–35.
55. Algaba A, Linares PM, Fernández-Contreras ME, *et al.* Relationship between levels of angiogenic and lymphangiogenic factors and the endoscopic, histological and clinical activity, and acute-phase reactants in patients with inflammatory bowel disease. *J Crohn's Colitis* 2013:e569–79.
56. Candia E, Díaz-Jiménez D, Langjahr P, *et al.* Increased production of soluble TLR2 by lamina propria mononuclear cells from ulcerative colitis patients. *Immunobiology* 2012;217:634–42.
57. Hart AL, Al-Hassi HO, Rigby RJ, *et al.* Characteristics of intestinal dendritic cells in inflammatory bowel diseases. *Gastroenterology* 2005;129:50–65.
58. Andoh A, Fujiyama Y, Kimura T, *et al.* Increased expression of decay-accelerating factor [CD55] in the inflamed mucosa of patients with ulcerative colitis. *Pathophysiology* 1998;5:105–10.
59. Sugihara T, Kobori A, Imaeda H, *et al.* The increased mucosal mRNA expressions of complement C3 and interleukin-17 in inflammatory bowel disease. *Clin Exp Immunol* 2010;160:386–93.
60. Barnett MP, McNabb WC, Cookson AL, *et al.* Changes in colon gene expression associated with increased colon inflammation in interleukin-10

- gene-deficient mice inoculated with *Enterococcus* species. *BMC Immunol* 2010;11:39.
61. Russ AE, Peters JS, McNabb WC, *et al.* Gene expression changes in the colon epithelium are similar to those of intact colon during late inflammation in interleukin-10 gene deficient mice. *PLoS One* 2013;8:e63251.
  62. te Velde AA, de KFE, Sterrenburg E, *et al.* Comparative analysis of colonic gene expression of three experimental colitis models mimicking inflammatory bowel disease. *Inflamm Bowel Dis* 2007;13:325–30.
  63. Foell D, Frosch M, Sorg C, Roth J. Phagocyte-specific calcium-binding S100 proteins as clinical laboratory markers of inflammation. *Clin Chim Acta* 2004;344:37–51.
  64. Nacken W, Roth J, Sorg C, Kerkhoff C. S100A9/S100A8: Myeloid representatives of the S100 protein family as prominent players in innate immunity. *Microsc Res Tech* 2003;60:569–80.
  65. Burri E, Beglinger C. The use of fecal calprotectin as a biomarker in gastrointestinal disease. *Expert Rev Gastroenterol Hepatol* 2013;8:197–210.
  66. Smith LA, Gaya DR. Utility of faecal calprotectin analysis in adult inflammatory bowel disease. *World J Gastroenterol* 2012;18:6782–9.
  67. Nielsen OH, Gionchetti P, Ainsworth M, *et al.* Rectal dialysate and fecal concentrations of neutrophil gelatinase-associated lipocalin, interleukin-8, and tumor necrosis factor- $\alpha$  in ulcerative colitis. *Am J Gastroenterol* 1999;94:2923–8.
  68. Chassaing B, Srinivasan G, Delgado MA, Young AN, Gewirtz AT, Vijay-Kumar M. Fecal lipocalin 2, a sensitive and broadly dynamic non-invasive biomarker for intestinal inflammation. *PLoS One* 2012;7:e44328.
  69. Ostvik AE, Granlund AV, Torp SH, *et al.* Expression of Toll-like receptor-3 is enhanced in active inflammatory bowel disease and mediates the excessive release of lipocalin 2. *Clin Exp Immunol* 2013;173:502–11.
  70. Thomas DD, Ridnour LA, Isenberg JS, *et al.* The chemical biology of nitric oxide: Implications in cellular signaling. *Free Radic Biol Med* 2008;45:18–31.
  71. Sohn JJ, Schetter AJ, Yfantis HG, *et al.* Macrophages, nitric oxide and microRNAs are associated with DNA damage response pathway and senescence in inflammatory bowel disease. *PLoS One* 2012;7:e44156.
  72. Kolios G, Valatas V, Ward SG. Nitric oxide in inflammatory bowel disease: a universal messenger in an unsolved puzzle. *Immunology* 2004;113:427–37.
  73. Dhillon SS, Mastropaolo LA, Murchie R, *et al.* Higher activity of the inducible nitric oxide synthase contributes to very early onset inflammatory bowel disease. *Clin Transl Gastroenterol* 2014;5:e46.
  74. McCafferty DM, Sihota E, Muscara M, Wallace JL, Sharkey KA, Kubes P. Spontaneously developing chronic colitis in IL-10/iNOS double-deficient mice. *Am J Physiol Gastrointest Liver Physiol* 2000;279:G90–9.
  75. Krieglstein CF, Anthoni C, Cerwinka WH, *et al.* Role of blood- and tissue-associated inducible nitric-oxide synthase in colonic inflammation. *Am J Pathol* 2007;170:490–6.
  76. Ahuja SK, Murphy PM. The CXC chemokines growth-regulated oncogene [GRO]  $\alpha$ , GRO $\beta$ , GRO $\gamma$ , neutrophil-activating peptide-2, and epithelial cell-derived neutrophil-activating peptide-78 are potent agonists for the type B, but not the type A, human interleukin-8 receptor. *J Biol Chem* 1996;271:20545–50.
  77. Atreya R, Neurath MF. Chemokines in inflammatory bowel diseases. *Dig Dis* 2010;28:386–94.
  78. Bain CC, Mowat AM. The monocyte-macrophage axis in the intestine. *Cell Immunol* 2014;291:41–8.
  79. Mowat AM, Bain CC. Mucosal macrophages in intestinal homeostasis and inflammation. *J Innate Immun* 2011;3:550–64.
  80. Turk R, 't Hoen PA, Sterrenburg E, *et al.* Gene expression variation between mouse inbred strains. *BMC Genomics* 2004;5:57.
  81. Holgersen K, Dobie R, Farquharson C, *et al.* Piroxicam treatment augments bone abnormalities in interleukin-10 knockout mice. *Inflamm Bowel Dis* 2015;21:257–66.
  82. Tarlton JF, Whiting CV, Tunmore D, *et al.* The role of up-regulated serine proteases and matrix metalloproteinases in the pathogenesis of a murine model of colitis. *Am J Pathol* 2000;157:1927–35.
  83. Hansen CH, Nielsen DS, Kverka M, *et al.* Patterns of early gut colonization shape future immune responses of the host. *PLoS One* 2012;7:e34043.
  84. Reading NC, Kasper DL. The starting lineup: key microbial players in intestinal immunity and homeostasis. *Front Microbiol* 2011;2:148.
  85. Moore KW, de Waal MR, Coffman RL, O'Garra A. Interleukin-10 and the interleukin-10 receptor. *Annu Rev Immunol* 2001;19:683–765.
  86. Berg DJ, Zhang J, Weinstock JV, *et al.* Rapid development of colitis in NSAID-treated IL-10-deficient mice. *Gastroenterology* 2002;123:1527–42.
  87. Hale LP, Gottfried MR, Swidsinski A. Piroxicam treatment of IL-10-deficient mice enhances colonic epithelial apoptosis and mucosal exposure to intestinal bacteria. *Inflamm Bowel Dis* 2005;11:1060–69.
  88. Maloy KJ, Powrie F. Intestinal homeostasis and its breakdown in inflammatory bowel disease. *Nature* 2011;474:298–306.